VULNERABILITY OF HOUSES AND PERSONS UNDER AVALANCHE IMPACT – THE AVALANCHE AT LONGYEARBYEN ON 2015-12-19

Dieter Issler*, Árni Jónsson, Peter Gauer, and Ulrik Domaas

Norwegian Geotechnical Institute, Oslo, Norway

ABSTRACT: This study uses data from the avalanche that killed two persons and destroyed eleven essentially identical wood-frame houses in Longyearbyen, Svalbard, on 2015-12-19. The avalanche is back-calculated with a dynamical model to estimate the spatial pressure distribution. For each affected building, the structural damage is categorized according to the remaining degree of protective function. However, relating the damage to the impact pressure is complicated by unusual features of this event. Finally, the fraction of inhabitants of each building who were injured or killed is related to the degree of structural damage instead of the usually used indicators pressure or velocity. In this way, it will be possible to compare and combine data from different building types and events to improve the estimate of the vulnerability of persons inside buildings against snow avalanches. Such vulnerability functions are needed for quantitative avalanche risk analysis in the context of planning mitigation measures or for legislative purposes. The data from this one event is not sufficient for establishing these functions, but the study will be extended to other events on which sufficiently detailed information is available.

1   INTRODUCTION

For some twenty years, economic limitations have brought about a paradigm shift in the management of natural hazards: Increasingly often, mitigation projects are prioritized according to their cost/benefit ratio. The notion of risk R as a measure of the expected damage per unit time plays a central role in this approach. For a given scenario S, it is the product of the occurrence probability $P(S)$, the degree of exposure E of objects or persons, and their vulnerability $V(S)$. For the total risk, one sums over scenarios: $R = \sum_S P(S)EV(S)$.

Quantitative risk analysis thus requires knowledge of all three factors. The exposure E is usually easiest to determine and can often be assumed to be independent of the scenario S. In the case of gravity mass movements like snow avalanches, a scenario can usually be defined as an avalanche exerting a certain maximum pressure at a given location; in some cases, the flow depth and the pressure profile may need to be considered as well. To determine $P(S)$, one may analyze histor-

ical events and climate statistics and simulate the avalanche flow with numerical or statistical tools.

There are different ways of defining the vulnerability of a construction or of persons. In the case of buildings, the expectation value of the repair or replacement cost is the vulnerability of concern to, e.g., insurance companies. For persons, the probability of sustaining severe injuries or death for a given scenario is often the most pertinent choice.

Obviously, the vulnerability of a building in a given scenario depends strongly on the type of construction and many details like the placement and size of doors and windows. One cannot expect vulnerability functions determined in the Alps (Barbolini et al., 2004; Bertrand et al., 2010; Bovet et al., 2011; Kobald, 2015; Schroll, 2015), where massive wood constructions, masonry or even reinforced concrete dominate, to be applicable to typical Norwegian homes with wooden frames and thin wooden hulls. It is immediately clear that these construction-related differences of building vulnerability V_b have a direct impact on the vulnerability V_p of persons inside buildings.

Our working hypothesis in this paper is that the dependence of V_p on building type can largely be factored out if one expresses it as a function $V_p(D)$ in terms of D, the degree of structural damage to the building. For survival of humans inside a building, the pressure outside or the construction material are not relevant per se—what counts is

*Corresponding author address:
Dieter Issler, Norwegian Geotechnical Institute, P.O. Box 3930 Ulleval Stadion, 0806 Oslo, Norway;
tel. +47-4698-7346; fax: +47-2223-0448;
e-mail: di@ngi.no

whether the building keeps the avalanche outside (small or no structural damage), or walls are broken in (moderate to considerable structural damage), or the entire structure collapses. For this reason, we define the vulnerability of buildings as the most likely degree of structural damage under a given avalanche pressure and the vulnerability of persons as the probability $V_p(D)$ of a person incurring death or severe injury if the building undergoes structural damage of degree D.

Clearly, the survival chance of an individual inside a building depends on many additional factors, e.g. age, health, location within the building at the time of impact, time to rescue and hospitalization. The latter two factors are especially important when a big avalanche catastrophe hits a small, remote community without the manpower and equipment needed for rapid rescue work. Rooms facing the mountainside typically suffer more severe damage than rooms facing the valley. In single-floor homes, bedrooms are often located on the impact side so that survival chances are significantly lower if the avalanche strikes at night. In most applications, one is interested in the average vulnerability. At its present stage, this study is limited to a single event and therefore is strongly affected by the specific circumstances. However, we expect these factors to average out when we apply the same methodology to a large number of additional events.

We define D according to the criteria in Tbl. 1, which builds on the classification developed by Grünthal (1998) for the European Macroseismic Scale. We modify that scale for our purpose to emphasize whether the rooms retain enough air volume that inhabitants are not injured, have enough air to breathe over a long period and are not in acute danger of hypothermia.

The validity of our factoring assumption and the usefulness of the criteria in Tbl. 1 need to be tested against real data. As a first step to this end, we analyzed data from the avalanche event in Longyearbyen, Svalbard, on 2015-12-19 (see (Hestnes and Bakkehøi, 2016; Brattlien et al., 2016; Jaedicke et al., 2016) for complementary information on this particular event). This study will be extended in the near future to include a number of avalanche events from Norway and Iceland. The analysis requires the following steps: (i) Reconstruction of the avalanche pressure and flow depth at the location of the affected houses, (ii) assessment of the degree of damage to the buildings and their inhabitants, and (iii) analysis of the relations between avalanche pressure, building type and degree of

Tbl. 1: Characterization of different degrees of damage to a building due to an avalanche impact.

Degree of damage D	Damage description
Category 1: 0–10%	All spaces intact to slightly skewed. Big voids and structure are stable.
Category 2: 10–40%	Impact side partly pushed in or skewed, limited voids at impact side, big voids at lee side, partly skewed/damaged internal walls. Snow/avalanche debris in 10–20% of the building.
Category 3: 40–70%	Impact side pushed in/collapsed, big voids approx. 50%, small voids due to snow avalanche debris approx. 20%. Snow/avalanche debris in at least 50% of the building.
Category 4: 70–90%	Impact side pushed in/collapsed, internal walls collapsed, no big voids, small voids due to snow avalanche debris approx. 20%. Snow/avalanche debris in at least 90% of the building.
Category 5: 90–100%	All spaces destroyed, (almost) no voids remain, large part of building scattered, most walls destroyed.

building damage D, and between D and the fate of the inhabitants.

2 SUMMARY OF THE AVALANCHE EVENT

On December 19, 2015 at 10:25 AM, a dry-snow avalanche with a drop height of about 90 m and a run-out angle of only 16° released from the northern shoulder of Sukkertoppen above the outskirts of the town of Longyearbyen, Svalbard. After a week without precipitation and temperatures mostly below −10°C, only about 20 cm of new snow fell that
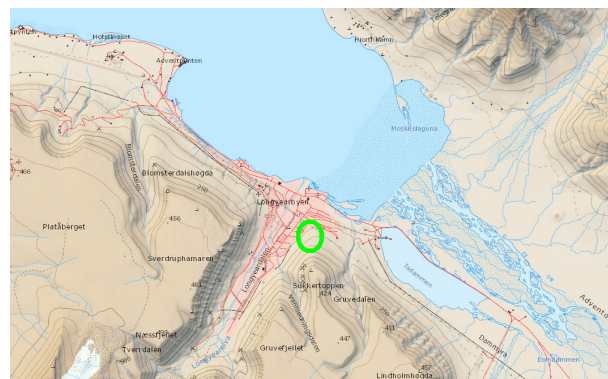

Fig. 1: Overview map of the Longyearbyen area, with the avalanche location marked by green circle.

Fig. 2: Overview of the destroyed houses from the release area. The house numbers are the same as those used in Tbl. 2. For the four houses in the upper row, their original locations are shown as rectangles.

day at -5 to $0\,^\circ$C at the nearby airport. Yet, the fracture height exceeded 3 m at some points and was close to 2 m on average, giving a release volume of approximately 25,000 m^3 and a fracture depth (normal to the terrain) of approx. 1.5 m. This was due to drifting snow under persistent strong south-easterly winds (up to 40 m s^{-1}). The avalanche width was 200 m, the maximum horizontal run-out 300 m.

The density and deposit depth were not measured. Considering the formation conditions, we estimate the density in the release area to 200–300 kg m^{-3}. The deposit density was likely similar, whereas the snow in the track and deposit area presumably was not much denser than 100 kg m^{-3}. With an estimated average deposit depth of 1.5–2 m over 20,000 m^2, the mass balance is consistent with the erodible snow available in the track.

The avalanche hit eleven of the landmark "*spisshus*" (pointed-gable houses) from the 1970s and stopped against a few larger two-story houses to the southwest without damaging them. The four *spisshus* in the uppermost row were displaced by up to 80 m (Fig. 2), and all eleven had to be dismantled afterwards. In total, 19 persons were inside the houses during the event. Eight of them had to be hospitalized, an adult and a toddler died. Inhabitants of similarly exposed houses in Longyearbyen were subsequently evacuated.

3 BACK-CALCULATION OF THE AVALANCHE

The back-calculations with the Voellmy-type model RAMMS::AVALANCHE v.1.6.20 were based on a digital terrain model with 2 m resolution, from which a computational grid with 5 m resolution was created. The observed release area was used with a uniform release depth of 2 m, i.e., somewhat more than the estimated average (Sec. 2). The simulation (Fig. 3) exhibits more lateral spreading, particularly in the northern corner of the deposit area, than observed. This may be due to a combination of lack of confinement at the lateral fracture lines, numerical diffusion and small-scale terrain features that are not resolved in the digital terrain model. The recommended parameter values (SLF, 2010) for a medium-size avalanche in high-alpine terrain with a return period of about 300 years lead to a run-out distance close to the observed one at the northern corner of the deposit area, while the run-out is overestimated by about 50 m in the corridor to the west of the destroyed houses. Without accounting for the braking effect of the two rows of houses, the simulated avalanche ran 0–50 m farther than observed.

Note that the cross-sectional profile along the upper side of the top row of houses (Fig. 4) indicates high values of velocity and flow depth at the location of house no. 21. However, no damage to this building is reported, and images show a moderate avalanche deposit against the house wall, contradicting the simulation result. We do not presently understand the reason for this discrepancy. As we will discuss in Sec. 4, the low degree of structural damage to, and short displacement of, house no. 16 indicates a similar effect along the northwestern edge of the path.

Parenthetically, we note that the run-out angle α (the angle from the fracture crown to the tip
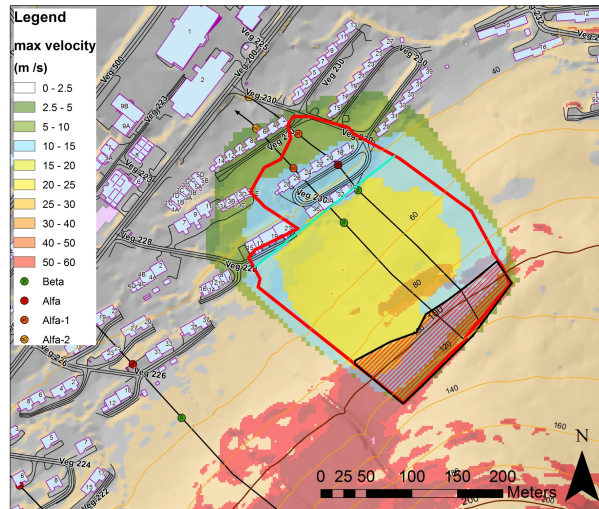
Fig. 3: Distribution of maximum velocity from numerical simulation of the 2015-12-19 Longyearbyen avalanche with RAMMS. The hatched area is the observed release area that was used in the simulation. See the text for the initial conditions and the parameter choices. The red line indicates the observed avalanche boundary, the cyan line corresponds to the profile of Fig. 4.

of the deposit) is very small at 16°. According to the topographical-statistical α-β model (Lied and Bakkehøi, 1980), calibrated against some 200 events of Norwegian avalanche events with long return periods ("extreme avalanches"), this run-out angle is about 2° or one standard deviation below the expectation value for an average track inclination of about 20.5°. This fits well with many other observations of small, long-runout avalanches on Svalbard (E. Hestnes, personal comm.) and the tendency of the α-β model to underestimate the run-out of small avalanches (with drop heights less than 200–300 m), which we have noted repeatedly in consulting work and also was confirmed by Wagner (2016). On the other hand, dynamical models like RAMMS often seem to perform better in such situations.

Given the limited length of this avalanche, the calibration of RAMMS recommended by SLF is expected to also model the avalanche velocities reasonably. The simulated speed at the top row of houses is 12–15 m s^{-1}, which appears plausible (Fig. 4). Unfortunately, there are no measurements of the deposit depth distribution, but again, at 1.5–2 m the simulated values are close to what we estimated from the available photos and the impressions gathered by one of us (U.D.) during field work two weeks after the disaster.
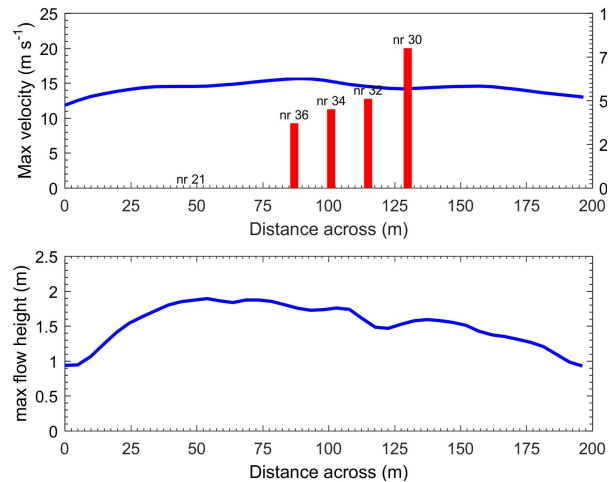

Fig. 4: Profiles of maximum velocity and flow height along the blue line in Fig. 3, from SW to NE.

In order to assess the action of the avalanche on the buildings, the flow depth and pressure (including their time evolution) are more relevant than the deposit depth. In this regard, the Voellmy model gives limited information because it assumes constant density of the snow masses from release to stop. Assuming a density ρ ≈ 300 kg m^{-3}, corresponding to the estimated release density, would indicate an impact pressure $p \approx \rho u^2 \approx$ 40–70 kPa against the upper row of houses. However, there are some circumstances that lead us to suspect that the real pressure may have been lower: (i) A mobile-phone video of the event is available, and despite the darkness, it shows a powder-snow cloud (of relatively low density) passing over the settlement. (ii) Judging from some photos, the deposit appears to be fairly thin in the opening between the destroyed houses and the unscathed ones to the south-west (near the left edge of Fig. 2). (iii) The snow was wind-packed only in the release area, whereas the density farther down the track was not much more than 100 kg m^{-3}. These considerations suggest that this avalanche was partly fluidized, so that the front density at impact may have been in the range 100–200 kg m^{-3}. Unless the fluidization increased the front velocity at impact beyond 15 m s^{-1}, the peak pressure would then have been 15–45 kPa (against wide solid walls).

Another important question concerns the spatial variability of the flow depth and pressure. Figure 4 shows a cross-sectional profile of the maximum flow-depth and velocity across the width of the avalanche at the location of the upper row of houses. Superposing the rafting distance of the houses at their respective locations, one sees that

Fig. 5: Detailed views of the damaged houses (extracted from Fig. 2). The numbers correspond to those in Tbl. 2 and Fig. 2.

there is no clear correlation between the observed rafting distance of the houses and the simulated avalanche properties at their locations. This can be due to (i) shortcomings in the simulation, (ii) differences in the weight and attachment of the houses, or (iii) the presence of obstacles like cars and other houses. Reason (i) is hinted at by the fact that the larger two-story house 21 was not damaged, despite the simulated velocity being almost the same as at the destroyed houses (the more robust construction of this building likely also contributed, however). The second reason presumably also played a role since the freeboard between the ground and the floor of the houses almost certainly differed between houses due to terrain irregularity. This determines how much snow could penetrate underneath the houses and much lift they experienced from below. The third reason cannot be dismissed either—house no. 36 was abruptly stopped by no. 28, nos. 26 and 24 stopped no. 34, and nos. 24 and 22 joined forces to stop no. 32. House no. 30 crashed squarely into no. 20, which was not inhabited at that point and thus may have

been about 5 t lighter than the other houses. This may explain why no. 20 offered less resistance and no. 30 traveled farthest.

4 PRELIMINARY DAMAGE ANALYSIS

Longyearbyen's *spisshus* differ in some important respects from standard Norwegian wood-frame houses: The houses are arranged in two rows (four in the upper row, seven in the lower), and neighboring houses are linked with a lightly built, 5–7 m long appendix that serves as wind shelter for the house entrance and as storage room in some houses, but is elaborated into a living or bedroom in others—particularly in the upper row (houses 30– 36). Due to the active layer above the permafrost, each house was supported by 15 wooden piles that protruded on average about 1 m over the ground surface. Three 9 m long wooden beams oriented in the flow direction of the avalanche and spaced 4 m apart, were tied to the piles with metal straps. The floor plate of the houses was weakly fixed to this foundation. Detailed construction plans are lost,

but it appears that the first and second stories were prefabricated separately, the former being like a box with fairly stiff floor, ceiling and walls, and the latter having the shape of an inverted U. The floor and roof consist of closely spaced wood rafters on wood studs. Lumbers of dimension $3.4 \times 15 \, \text{cm}^2$, typically spaced 0.6 m apart, form the wooden frame. Floor, roof and shear wall diaphragms consist of straight wood sheathing or 2 cm thick woodchip boards. Wood-frame diaphragms and shear walls provide considerable resistance against forces along these walls. The structural strength of the *spisshus* was likely higher than that of a typical Norwegian wood-frame dwelling. A rough estimate of the mass of the houses yields 20–25 (metric) tons.

We have scant information on the structure of the connecting one-story structures between houses. Based on images, particularly the left-most of the middle row of Fig. 5, we conjecture that they were built upon a floor plate of some stiffness and that the roof also had a certain degree of stiffness. It is unclear whether all these connecting structures had side walls of their own and how strongly they were connected to the adjacent houses. The strength of these structures is probably somewhat inferior to that of a typical Norwegian wood-frame home. The avalanche impact completely destroyed most of the connecting structures between houses. Several of those in the upper row were torn to pieces and scattered over a considerable area, while those in the lower row were partly torn apart by their adjacent houses moving in different directions or by impact with a house from the upper row.

House no. 20 in the lower row was sheltered from direct avalanche impact, but hit essentially square on by no. 30. The damage was slight, apparently because the impact force could be transferred to the stiff floor and roof plates and the longitudinal walls. The house was nevertheless promptly dismantled because it came to rest on the access street to the third row of houses. House no. 28 received more damage because it was hit by no. 36 at an angle. Similarly, nos. 24 and 26 suffered considerable damage because their upper sides were hit by the corners of nos. 32 and 34.

The elevated position of the houses and their weak fixation to the foundation caused the avalanche to partly push, partly lift the houses from their foundations, sweeping them up to 80 m downstream. In particular, there was virtually no pile-up of avalanche debris behind houses no. 30, 32 and 36 (Fig. 5)—they seem to have been rafted along. Interestingly, these three houses show similar dam-

age to the outer hull at the sides of the lower gable area. This rafting generally reduced the structural damage in the upper row, but houses in the lower row were damaged more severely by collisions between houses than by the avalanche itself.

The avalanche impacted the directly exposed houses of the upper row over a height of 0.5–1.5 m and a width of 8 m. As discussed in Sec. 3, we estimate the pressure to 15–45 kPa, leading to a pressure force in the wide range 120–540 kN, with 300–400 kN the most plausible value. The net force in the range 175–325 kN would then induce an initial acceleration of the order of 7–13 m s^{-2}. Within approx. 2–4 s, the houses would attain a speed close to that of the flowing snow. Accelerating the houses must have reduced the avalanche speed around them considerably: The mass penetrating underneath a house or pushing from behind was likely about $200 \, \text{m}^3 \times (100\text{–}200) \, \text{kg m}^{-3} = (2\text{–}4) \times 10^4$ kg, i.e., similar to the mass of the house. Accordingly, we expect the flow to be slowed down to about half its speed without houses present, i.e., to 3–5 m s^{-1} about midway between the two rows of houses.

Some of the surviving inhabitants of the lower row reported that the avalanche impact itself was not particularly violent—persons or objects were not thrown around. This limits the acceleration to 1–2 m s^{-2} and the net force (pressure from the avalanche or impacting house minus resistance) to about 25–50 kN. It is difficult to estimate the resistance force, to which different factors contributed: fixation to the foundation, friction against the foundation, plowing of the snow ahead of the houses. Assuming an effective friction coefficient of 0.3–0.5 for a ballpark estimate, we obtain 75–125 kN; thus, the impact force may have been of the order of 100–175 kN.

We estimate the impact speed of the upper-row houses onto the lower-row houses to 1–3 m s^{-1}. Modeling the impact as a totally inelastic collision and assuming the houses were deformed by $\Delta s \approx 5$ cm, the impact time was of the order of 50–100 ms. The momentum transfer was $\Delta J = \frac{1}{2} M_{\text{house}} v_{\text{house}} \approx (1\text{–}4) \times 10^4$ kg m s^{-1}. The time-averaged impact force thus amounts to $\overline{F}_{\text{impact}} = \Delta J / \Delta t = 100\text{–}800$ kN. The lower limit of this range agrees well with the estimate obtained above from the absence of strong acceleration. The upper limit, on the other hand, would almost certainly cause the impacted walls to shatter and thus would increase the deformation distance and time drastically. A detailed analysis of the structural response of such houses would be needed to confirm

Tbl. 2: Overview of houses hit by the 2015 Longyearbyen avalanche, with degree of damage ($D_{1,2}$) to 1st/2nd floor, number of adults and children present (1st/2nd floor) and number of injured adults/children. D_1 refers either to the 1st floor or to the annex room, depending on where people were present.

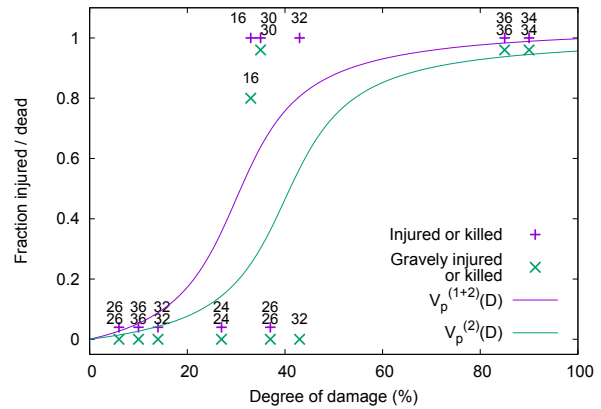| No.	D_1 / D_2	Adults	Chld.	Moderate injury	Grave injury/ death
16	30 / 0	4 / 0	1 / 0	1 / 0	3 / 1
18	30 / 10	0 / 0	0 / 0	– / –	– / –
20	10 / 0	0 / 0	0 / 0	– / –	– / –
22	20 / 0	0 / 0	0 / 0	– / –	– / –
24	60 / 30	0 / 1	0 / 0	0 / –	0 / –
26	40 / 10	0 / 2	2 / 0	0 / 0	0 / 0
28	40 / 10	0 / 0	0 / 0	– / –	– / –
30	35 / 0	1 / 0	0 / 0	0 / –	1 / –
32	40 / 10	2 / 0	0 / 1	2 / 0	0 / 0
34	90 / 60	1 / 0	0 / 0	0 / –	1 / –
36	85 / 10	0 / 2	2 / 0	0 / 0	0 / 2

Fig. 6: Vulnerability as a function of the degree of (structural) damage: Fraction of moderately or severely/lethally injured persons in the 2015 Longyearbyen avalanche. The data is not differentiated according to age.

these conclusions, but at least they appear reasonably consistent with the available observations. The special circumstances of this event (shear forces due to rapid acceleration of the houses, rafting over long distances and collisions between houses) make the elaboration of a vulnerability function a challenging task.

5 VULNERABILITY FUNCTION FOR PERSONS

Given the large uncertainties in assessing the degree of damage and the decisive role that uncontrollable circumstances play in avalanche accidents, we cannot hope to arrive at a practically usable vulnerability function with data from this single event. It is nevertheless of interest to carry out the analysis in order to detect potential shortcomings of the methodology.

The basis data for plotting the vulnerability of persons in buildings against the degree of damage is given in Tbl. 2. In creating Fig. 6, we combined adults and children due to the small number of data points. On the other hand, we distinguished between people on the first floor of the house proper and the annex because the degree of damage is 90–100% for the latter, but rarely more than 50% for the former. The adult and child who lost their lives both were in an annex. In order to make the plot easier to comprehend, we plotted the *sum* of moderately, gravely and mortally injured people instead of the moderately injured ones only; in this way, the curve is always coincident with or above the one for gravely or mortally injured victims, and the difference between the curves correpsonds to the fraction of moderately injured persons. Moreover, we slightly changed the degree of damage and the number of affected persons in order to resolve overlaps of data points in the plot.

The most natural way of categorizing the damage to humans in a situation with low statistics would perhaps be in terms of "unharmed" – "injured" – "killed". We chose instead the categories "unharmed or lightly injured" – "moderately injured" – "gravely injured or killed". Our rationale for doing so is that often a chance combination of circumstances determines whether avalanche victims will survive or not if they are severely injured, e.g., physical constitution, the presence of furniture that can protect or kill, the proximity and equipment of rescuers, medical equipment, etc. Yet another approach would be to quantify the severeness of injuries on a scale from 0 to 1, with 1 corresponding to fatal injuries. In that way, the sample size (the number of persons present on the same floor of the building) is increased and there is only one function to deal with, but this approach raises the touchy (and difficult) question of how to weigh injuries against loss of life.

In buildings that are not occupied by a large number of persons, the fraction of injured persons has a strong tendency to be either 0 or 1. This is exemplified by our data set (Fig. 6): Except in one case (house no. 16), either all persons present on

the same floor of the house were injured, or all were unscathed. (As Tbl. 2 shows, there were five cases with two persons present on the same floor.)

The records of the rescue operations hint that snow penetrating into houses may present an even larger danger to the lives of the inhabitants than the criteria in Tbl. 1 suggest: Even though the structural damage to house no. 16 was minor, four persons in the kitchen on the first floor were fully buried in the snow masses and could have lost their lives, had they not been rescued quickly.

Our data set is too tenuous and incomplete for firm conclusions about the shape of the vulnerability curves $V_p^{(2)}(D)$ for grave or lethal injuries and $V_p^{(1+2)}(D)$ for moderate to lethal injuries. We nevertheless venture to show such curves in Fig. 6, but we caution that they were adjusted manually to guide the reader's eye and not determined by a comprehensive statistical analysis, for which well-established methods exist, see e.g. (Porter, 2016) for a pedagogical introduction.

6   DISCUSSION AND CONCLUSIONS

The 2015 Longyearbyen avalanche brought tragedy to this high-Arctic town in the middle of the long winter darkness. It has, however, raised the awareness for the pervasive natural hazards that threaten this community, hopefully leading to better protection in the future. It also presented a rare opportunity for studying how wood-frame homes interact with a substantial, yet not gigantic avalanche. Even under almost identical conditions with regard to avalanche parameters and building structure, significant differences were observed concerning both the degree of structural failure and the survival chances of the inhabitants. Thus, statistical analysis necessarily has to play an important role in the elaboration of vulnerability functions.

Our data set is by far too small to allow firm conclusions on the form of the vulnerability functions, but the trends found appear reasonable, as exemplified by Fig. 6. As further events like the 1995 avalanche catastrophes of Suðavík and Flateyri in Iceland are analyzed in this way, the criteria and percentages given in Tbl. 1 will certainly need adjustment. But if the loss of protective capacity of the building indeed proves to be a useful independent variable for the vulnerability curves for people, it will be interesting to compare (i) the curves for snow avalanches against different building types, and (ii) the curves obtained from different natural hazards like slushflows, debris flows, tsuanmis, and earthquakes. Especially for the latter two, there is extensive statistical data available from the giant catastrophes of the past few decades.

REFERENCES

Barbolini, M., Cappabianca, F., and Savi, F. (2004). Risk assessment in avalanche-prone areas. *Annals of Glaciology*, 38:115–122.

Bertrand, D., Naaim, M., and Brun, M. (2010). Physical vulnerability of reinforced concrete buildings impacted by snow avalanches. *Natural Hazards and Earth System Sciences*, 10(7):1531–1545.

Bovet, E., Chiaia, B., De Biagi, V., and Frigo, B. (2011). Pressure of snow avalanches against buildings. *Applied Mechanics and Materials*, 82:392–397.

Brattlien, K., Hestnes, E., and Domaas, U. (2016). The Svalbard fatal accident 19th December 2015 -– the acute phase. In *Proc. of the International Snow Science Workshop 2016, Breckenridge*. In preparation.

Grünthal, G. (1998). European macroseismic scale 1998 EMS-98. Cahiers du Centre Européen de Géodynamique et de Séismologie 15, European Seismological Commission, Luxembourg.

Hestnes, E. and Bakkehøi, S. (2016). Longyearbyen, Svalbard – vulnerability and risk managment of an Arctic settlement under changing climate – a challenge to authorities and experts. In *Proc. of the International Snow Science Workshop 2016, Breckenridge*. In preparation.

Jaedicke, C., Hestnes, E., Bakkehøi, S., Mørk, T., and Brattlien, K. (2016). Forecasting the fatal Longyearbyen avalanche: Possibilities and challenges. In *Proc. of the Intl. Snow Science Workshop 2016, Breckenridge*. In preparation.

Kobald, J. (2015). Entwicklung von Kriterien zur Bestimmung von Gebäudeschutzklassen – Sammlung und Analyse von durch Steinschlag und Lawinen beschädigten Gebäuden. Master's thesis, Dept. of Civil Engineering and Natural Hazards, University of Natural Resources and Life Sciences, Vienna, Austria. no. 13417.

Lied, K. and Bakkehøi, S. (1980). Empirical calculations of snow-avalanche run-out distance based on topographic parameters. *Journal of Glaciology*, 26(94):165–177.

Porter, K. E. (2016). A Beginner's Guide to Fragility, Vulnerability, and Risk. Available athttp://spot.colorado.edu/ porterka/Porter-beginners-guide.pdf, accessed 2016-08-23.

Schroll, L. (2015). Schadwirkung von Lawinen. Master's thesis, Faculty of Technical Sciences, University of Innsbruck, Innsbruck, Austria.

Wagner, P. (2016). Kalibrierung des α-β-Modells für das Ermitteln der Auslauflänge von kleinen und mittleren Lawinen. Master's thesis, Inst. for Mountain Risk Engineering, Univ. of Natural Resources and Life Sciences BOKU, Vienna, Austria. In German, with English summary.